

Model Predictive Robustness of Signal Temporal Logic Predicates

Yuanfei Lin^{*,1}, Haoxuan Li^{*,2}, and Matthias Althoff¹

Abstract—The robustness of signal temporal logic not only assesses whether a signal adheres to a specification but also provides a measure of how much a formula is fulfilled or violated. The calculation of robustness is based on evaluating the robustness of underlying predicates. However, the robustness of predicates is usually defined in a model-free way, i.e., without including the system dynamics. Moreover, it is often nontrivial to define the robustness of complicated predicates precisely. To address these issues, we propose a notion of model predictive robustness, which provides a more systematic way of evaluating robustness compared to previous approaches by considering model-based predictions. In particular, we use Gaussian process regression to learn the robustness based on precomputed predictions so that robustness values can be efficiently computed online. We evaluate our approach for the use case of autonomous driving with predicates used in formalized traffic rules on a recorded dataset, which highlights the advantage of our approach compared to traditional approaches in terms of expressiveness. By incorporating our robustness definitions into a trajectory planner, autonomous vehicles obey traffic rules more robustly than human drivers in the dataset.

I. INTRODUCTION

Formal methods are crucial for specifying and verifying the behaviors of autonomous robotic systems [1]. Temporal logic, such as linear temporal logic (LTL) [2], metric temporal logic (MTL) [3], and signal temporal logic (STL) [4], allows one to specify safety properties and unambiguous tasks for a system over time. A prominent example is the formalization of traffic rules for autonomous vehicles on which we focus in this paper, e.g., “A vehicle must keep a safe distance from others in its lane to avoid collisions in the event of unexpected stops.” MTL and STL are additionally equipped with quantitative semantics, i.e., robustness (aka robustness degree) [5], [6], returning the degree of satisfaction or violation of a system with respect to a given specification. In this work, we focus on specifications formalized in STL since one can easily represent discrete-time MTL formulas in STL [7] and recent research on improving the robustness mainly addresses STL (see Sec. I-A.2).

The robustness of predicates is an essential building block for evaluating the robustness of STL formulas. However, the robustness of STL predicates is typically defined in a model-free manner, i.e., without considering the underlying system dynamics. As a result, the existing STL robustness does not accurately reflect the degree of satisfaction of predicates

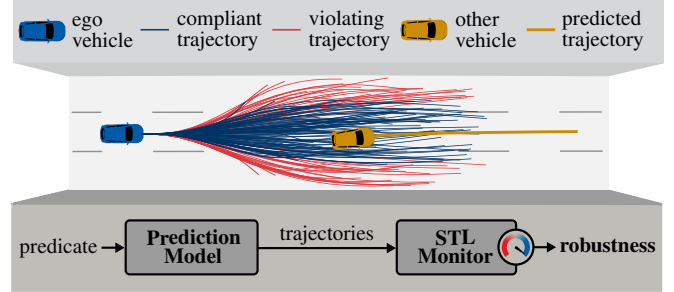


Fig. 1: Scheme of model predictive robustness computation for the predicate `in_same_lane`. The prediction model generates a finite set of trajectories for all rule-relevant vehicles within a certain time period, of which the rule compliance is checked by the STL monitor. The robustness is calculated based on the future probability of satisfying the predicate.

or rules. In addition, formulating a precise definition of robustness in a unified way can be challenging, especially when not taking into account the unique characteristics and features of the models. This issue is addressed in this work by the general idea illustrated in Fig. 1.

A. Related Work

Our robustness definition aims to facilitate online planning and control with temporal logic specifications. Subsequently, we present related works on specification formalization, model-free robustness, and nonlinear regression approaches.

1) *Specification Formalization*: The development of autonomous vehicles requires planning and control to fulfill formal specifications. Several publications formalize traffic rules for interstates [3], [8], intersections [9], and waterways [10] in MTL. They use parameterizable Boolean predicates and functions in higher-order logic to specify basic elements of rule specifications. In [4], [11], [12], safety requirements are specified in STL together with the robustness definition for formal verification and controller synthesis.

2) *Model-free Robustness*: The robustness of STL is typically nonconvex and nondifferentiable, see, e.g., [6]. Therefore, it is generally difficult to deploy fast gradient-based optimization algorithms for online usage, such as optimization-based trajectory planning for autonomous vehicles [13]. Many new extensions for STL robustness have been proposed to address this issue. In [14]–[17], smooth approximations are applied to make the robustness differentiable. To handle complex specifications efficiently, [18] considers STL formulas over convex predicates. However, these works only refine the robustness calculation for temporal and logical operators while using affine functions to compute the robustness of predicates.

^{*} The first two authors have contributed equally to this work.

¹Yuanfei Lin and Matthias Althoff are with the School of Computation, Information and Technology, Technical University of Munich, 85748 Garching, Germany.

²Haoxuan Li is with the School of Engineering and Design, Technical University of Munich, 85748 Garching, Germany.

{yuanfei.lin, haoxuan.li, althoff}@tum.de

For uncertain and changing environments, a probabilistic variant of STL is proposed to express safety constraints on random variables and stochastic signals in [19]–[21]. Similarly, Lee *et. al.* [22] extend STL with uncertain events as predicates to formulate a controller synthesis problem as probabilistic inference. Meanwhile, the authors in [23] model the risk of violating safety specifications over a random variable. However, these works only assess the signal in the form of probability distributions and do not evaluate the system or model’s ability to handle uncertainties or perturbations using stochastic methods, which our work aims to address.

3) *Nonlinear Regression*: Supervised learning algorithms, e.g., regression and classification, have been used to model relationships between variables to improve prediction accuracy and computational efficiency. For safety-critical applications, Gaussian processes (GPs) [24] have drawn more and more attention since they are flexible and powerful for small-data problems. In addition, GP regression can provide uncertainties for its prediction, which is used to improve the safety and robustness of model predictive control in [25]–[27]. In this regard, we are inspired by the regression approach described in [28], where a GP model is used for estimating the robustness of STL specifications including levels of evaluation uncertainty. However, a more general observation space for autonomous driving is adapted for regression in this paper.

B. Contributions

We present a novel approach to determine the robustness of STL predicates, where the model capability for rule compliance is explicitly considered. When defining a new predicate, the robustness can be directly computed based on its Boolean evaluation instead of relying on manually tuned heuristics. In particular, our contributions are:

- 1) proposing for the first time a systematic robustness measure for STL predicates based on predictive models;
- 2) using GP regression to learn robustness with comprehensive input features for online applications; and
- 3) demonstrating the effectiveness of our robustness definition on formalized traffic rules with real-world data.

The remainder of this paper is organized as follows: In Sec. II, required preliminaries and formulations are introduced. Sec. III provides an overview of the model predictive robustness definition and computation. In Sec. IV, GP regression is presented to learn the robustness of predicates. We demonstrate the benefits of our method by numerical experiments in Sec. V, followed by conclusions in Sec. VI.

II. PRELIMINARIES

A. System Description and Notation

We model the dynamics of vehicles as discrete-time systems:

$$x_{k+1} = f(x_k, u_k), \quad (1)$$

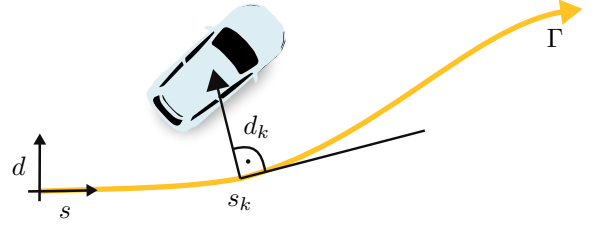


Fig. 2: A curvilinear coordinate system aligned with the reference path Γ .

where $x_k \in \mathbb{R}^{n_x}$ is the state, $u_k \in \mathbb{R}^{n_u}$ is the input, and the index $k \in \mathbb{N}_0$ is the discrete time step corresponding to the continuous time $t_k = k\Delta t$ with a fixed time increment $\Delta t \in \mathbb{R}_+$. We use a curvilinear coordinate system [29] that is aligned with a reference path Γ (e.g., the lane centerline), as shown in Fig. 2. The position of the vehicle at time step k is described by the arc length s_k along Γ and the orthogonal deviation d_k to Γ at s_k . The states and the inputs are bounded by sets of permissible values: $\forall k : x_k \in \mathcal{X}_k, u_k \in \mathcal{U}_k$. We denote a possible solution of (1) at time step $\tau \geq k$ by $\chi(\tau, x_k, u([k, \tau]))$ for an initial state x_k and an input trajectory $u([k, \tau])$. The set of possible state trajectories for the time interval $[k, \tau]$ is denoted as $\mathcal{X}_{[k, \tau]}$.

We introduce the following sets: $\mathcal{B} \subset \mathbb{N}_0$ is the set of indices referring to rule-relevant obstacles and $\mathcal{L} \subset \mathbb{N}_0$ contains the indices of the occupied lanes by a vehicle. $\mathcal{L}^c \in \mathcal{L}$ is the element of \mathcal{L} comprising the lane containing the vehicle center. The road boundary is denoted as b . Let \square be a variable, we denote its value associated with the ego vehicle, i.e., the vehicle to be controlled, by \square_{ego} and with other obstacles by \square_b , with $b \in \mathcal{B}$.

For regression models, we use feature variables containing the relevant vehicular and environmental information as the inputs $z \in \mathbb{R}^{n_z}$ and the corresponding robustness of predicates as the output $y \in \mathbb{R}$. With $n_p \in \mathbb{N}_{>0}$ input-output pairs, the training set is given by $\mathcal{D} = \{(z_i, y_i)\}_{i=1}^{n_p}$. The feature variables $z = o(\omega_k)$ are obtained via an observation function $o: \mathcal{X}_k^{|\mathcal{B}|+1} \rightarrow \mathbb{R}^{n_z}$, where the vector $\omega_k = [x_{\text{ego},k}, x_{0,k}, \dots, x_{|\mathcal{B}|-1,k}]^T \in \mathcal{X}_k^{|\mathcal{B}|+1}$ consists of the state vectors of the ego vehicle and other rule-relevant obstacles at time step k . The output predicted by the regression model is denoted as y^* .

B. Signal Temporal Logic

For traffic rule monitoring, we consider a discrete-time signal $\omega := \omega_0 \dots \omega_k \dots \omega_{n_\omega} \in \Omega$ representing a sequence of vectors ω_k , where the set Ω is a superset that includes all possible signals. Given formulas φ , φ_1 , and φ_2 , the STL syntax is defined as [7, Sec. 2.1]:

$$\varphi := p \mid \neg \varphi \mid \varphi_1 \vee \varphi_2 \mid \varphi_1 \mathbf{U}_I \varphi_2, \quad (2)$$

where $p := \alpha(\omega_k) > 0$ is an atomic predicate defined by the evaluation function $\alpha: \mathcal{X}_k^{|\mathcal{B}|+1} \rightarrow \mathbb{R}$, \neg and \vee are the Boolean *negation* and *disjunction* operators, respectively, and \mathbf{U}_I is the *until* operator requiring φ_1 to remain true until φ_2 becomes true in a time interval $I \subseteq \mathbb{N}_0$. Other logical

connectives and temporal operators can be constructed from (2) such as the *conjunction* operator $\varphi_1 \wedge \varphi_2 := \neg(\neg\varphi_1 \vee \neg\varphi_2)$ and the *future* (aka *eventually*) operator $\mathbf{F}_I \varphi := \top \mathbf{U}_I \varphi$ [7, Sec. 2.1].

To show whether an STL formula is satisfied with qualitative semantics, we introduce the characteristic function:

Definition 1 (Characteristic Function [6, Def. 1]):

The characteristic function $c : \Omega \times \mathbb{N}_0 \rightarrow \{-1, 1\}$ of an STL formula φ (cf. (2)) and a signal ω at time step k is defined as:

$$\begin{aligned} c_p(\omega, k) &:= \begin{cases} 1 & \text{if } \alpha(\omega_k) > 0, \\ -1 & \text{otherwise,} \end{cases} \\ c_{\neg\varphi}(\omega, k) &:= -c_\varphi(\omega, k), \\ c_{\varphi_1 \vee \varphi_2}(\omega, k) &:= \max(c_{\varphi_1}(\omega, k), c_{\varphi_2}(\omega, k)), \\ c_{\varphi_1 \mathbf{U}_I \varphi_2}(\omega, k) &:= \max_{\tau \in (k+I) \cap \mathbb{N}_0} \left(\min(c_{\varphi_2}(\omega, \tau), \min_{\tau' \in [k, \tau)} c_{\varphi_1}(\omega, \tau')) \right). \end{aligned} \quad (3)$$

For an exemplary calculation of the model-free STL robustness, we refer interested readers to [6, Def. 3].

C. Problem Formulation

Inspired by the metrics described in [15], [23], the robustness of STL predicates should follow the subsequent properties for its application to planning and control problems:

Property 1 (Soundness):

Positive robustness is a necessary and sufficient condition for satisfying the predicate; likewise, a signal has negative robustness for violating the predicate.

Property 2 (Smoothness):

The robustness is smooth with respect to its input almost everywhere¹ except on the satisfaction or violation boundaries where $\alpha(\omega_k) = 0$.

Property 3 (Monotonicity):

The robustness increases with a growing probability of satisfying the predicate and decreases otherwise.

The soundness and smoothness can be considered by following the requirements in [15, Thm. 1 and Prop. 1]. For monotonicity, the robustness needs to rely on dynamic models and predictive behaviors of the described system, which we call *model predictive robustness* since the idea is inspired by model predictive control [30] and model-based criticality measures [31]. In this work, we mainly focus on traffic rule predicates defined in higher-order logic, but our definition can be extended to other types of predicates.

III. MODEL PREDICTIVE ROBUSTNESS

In this section, model predictive robustness is first formally defined. Then we introduce a Bayesian representation of the predictive model. Afterwards, the overall algorithm for the computation of the robustness is presented, followed by its detailed description.

¹This is because smoothness across the entire domain is a too strict requirement for STL robustness [17, Sec. IV].

A. Definition

At time step $\tau \geq k$, we denote the predicted signal vector and characteristic function's output as ω'_τ and C_τ^p , respectively, which are modeled as random variables as their future evaluation is uncertain.

Definition 2 (Model Predictive Robustness):

The model predictive robustness ρ_p^{MP} considers the probability $P(\omega, k)$ that the output of the characteristic function is unchanged over a finite prediction horizon $h \in \mathbb{N}_0$ and is defined as:

$$\begin{aligned} \rho_p^{\text{MP}}(\omega, k) &:= \begin{cases} \frac{P(\omega, k) - \bar{P}_{+, \min}}{\bar{P}_{+, \max} - \bar{P}_{+, \min}} & \text{if } c_p(\omega, k) = 1, \\ -\frac{P(\omega, k) - \bar{P}_{-, \min}}{\bar{P}_{-, \max} - \bar{P}_{-, \min}} & \text{if } c_p(\omega, k) = -1, \end{cases} \\ \text{s.t. } P(\omega, k) &:= \frac{1}{h+1} \sum_{\tau=k}^{k+h} P(C_\tau^p = c_p(\omega, k)), \\ \bar{P}_{\pm, \max} &:= \max_{\bar{\omega} \in \Omega, \bar{k} \in \mathbb{N}_0} P(\bar{\omega}, \bar{k} \mid c_p(\bar{\omega}, \bar{k}) = \pm 1), \\ \bar{P}_{\pm, \min} &:= \min_{\bar{\omega} \in \Omega, \bar{k} \in \mathbb{N}_0} P(\bar{\omega}, \bar{k} \mid c_p(\bar{\omega}, \bar{k}) = \pm 1), \end{aligned} \quad (4)$$

where $\rho_p^{\text{MP}}(\omega, k)$ is normalized to the interval $[-1, 1]$ with the normalization values $\bar{P}_{\pm, \max} \in \mathbb{R}_0$ and $\bar{P}_{\pm, \min} \in \mathbb{R}_0$. Note that the normalization values can be approximated for online usage, e.g., from a dataset.

B. Prediction Model with Monte Carlo Simulation

To predict traffic rule satisfaction or violation, vehicle behaviors can be represented by probabilistic graphical models [32, Pt. I], e.g., dynamic Bayesian network [33]. The characteristic functions are computed by performing inference on the hidden variables. The probability of maintaining the value of the characteristic function at time step τ can be written as:

$$\begin{aligned} P(C_\tau^p = c_p(\omega, k)) &= \sum_{\omega'_\tau \in \Omega'_\tau} P(C_\tau^p = c_p(\omega, k) \mid \omega'_\tau) P(\omega'_\tau) \\ &= \sum_{\omega'_\tau \in \Omega'^c_\tau} P(\omega'_\tau), \end{aligned} \quad (5)$$

where Ω'_τ is the set of ω'_τ , $\Omega'^c_\tau \subseteq \Omega'_\tau$ is its subset satisfying $C_\tau^p = c_p(\omega, k)$, and $P(C_\tau^p = c_p(\omega, k) \mid \omega'_\tau)$ is either 0 or 1. However, it is nontrivial to obtain the exact distribution of the probability $P(\omega'_\tau)$ in (5) [34, Sec. V]. Instead, we employ Monte Carlo simulation to generate potential future behaviors of the ego vehicle [35, Sec. 1]. Meanwhile, we rely on predicted behaviors for other traffic participants since their movements are not within our power to dictate [36]. Note that such a choice is not mandatory and any other estimation method that interprets the true distribution suffices. The inaccuracy and uncertainty in the future behavior realizations are taken into account by introducing process deviation in the regression model, see Sec. IV. By assembling the obtained trajectories, the Monte Carlo estimation of the probability in

(5) can be calculated as the ratio of the number of predicted signal vectors in Ω'_τ to the size of Ω'_τ [35, Sec. 1]:

$$\sum_{\omega'_\tau \in \Omega'_\tau} P(\omega'_\tau) \approx \frac{|\Omega'_\tau|}{|\Omega'_\tau|}. \quad (6)$$

C. Overall Algorithm

Alg. 1 provides an overview of the computation of the model predictive robustness for traffic rule predicates. At time step k , we receive as input the predicate, the signal vector, and the prediction horizon. First, we randomly sample a set of trajectories $\chi_{\text{ego},[k,k+h]}$ for the ego vehicle based on its current state (line 1; cf. Sec. III-D). Afterward, if the predicate is associated with other traffic participants, i.e., $|\mathcal{B}| > 0$, their predicted trajectories $\chi_{\mathcal{B},[k,k+h]}$ are determined (line 3). When computing the robustness offline, we use their recorded trajectories, e.g., from a dataset. Then the set of all predicted signals $\Omega'_{[k,k+h]} := \Omega'_k \dots \Omega'_\tau \dots \Omega'_{k+h}$ is constructed by the two sets of trajectories (line 7). The last step is to compute the model predictive robustness by checking the relative frequency of rule-compliant or rule-violating predicted signals with the STL monitor (line 8).

Algorithm 1 COMPUTEMODELPREDICTIVEROBUSTNESS

Input: predicate p , signal ω at time step k , horizon h

Output: model predictive robustness ρ_p^{MP}

```

1:  $\chi_{\text{ego},[k,k+h]} \leftarrow \text{SAMPLEEGOTRAJ}(\omega_k, h)$  ▷ Sec. III-D
2: if  $|\mathcal{B}| > 0$  then
3:    $\chi_{\mathcal{B},[k,k+h]} \leftarrow \text{PREDICTOTHERTRAJ}(\omega_k, h)$ 
4: else
5:    $\chi_{\mathcal{B},[k,k+h]} \leftarrow \emptyset$ 
6: end if
7:  $\Omega'_{[k,k+h]} \leftarrow \text{CONSTRUCTSIGNAL}(\chi_{\text{ego},[k,k+h]}, \chi_{\mathcal{B},[k,k+h]})$ 
8:  $\rho_p^{\text{MP}} \leftarrow \text{STLMONITORING}(p, \Omega'_{[k,k+h]})$  ▷ (4), (6)
9: return  $\rho_p^{\text{MP}}$ 

```

D. Trajectory Sampling for the Ego Vehicle

Trajectories can be sampled either in control space or in state space [37] (see Fig. 3). The former generates trajectories through the forward simulation of the vehicle dynamics. In contrast, with the state-based strategy, the trajectories are obtained by connecting pairs of vehicle states, which helps to exploit environmental constraints to avoid unnecessary samples. Since we only consider structured environments and want to provide more reactive capabilities for the ego vehicle, the state-space sampling approach described in [38] is used.

As shown in Fig. 3b, a set of end states at time step $k+h$ are drawn uniformly from predefined sampling intervals in the curvilinear coordinate system along the reference path Γ . Alternative sampling distributions can be adapted if a specific pattern of the ego vehicle's behavior is known. Then trajectories are computed by connecting the end states with the current ego state at time step k using quintic polynomials. Afterward, the kinematic feasibility of the trajectories is

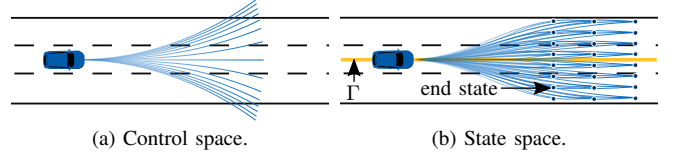


Fig. 3: Comparison of different sampling strategies for the ego vehicle.

checked, e.g., using the *CommonRoad Drivability Checker* [39], and the feasible ones are transformed from the curvilinear coordinate to the Cartesian frame as sampled trajectories for the ego vehicle.

IV. GAUSSIAN PROCESS REGRESSION

Determining the model predictive robustness is computationally expensive as well as noisy due to the sampling errors (cf. Sec. III-D). As motivated in Sec. I-A, we choose GP regression to learn the robustness.

A. Feature Variables and Robustness Prediction

A GP is a collection of random variables such that any finite subset of those variables is jointly Gaussian distributed [24, Def. 2.1]. The discriminative capabilities of GP regression models highly depend on the selection of the feature variables [24, Sec. 7.5]. We group the measurements of the feature variables z in four categories as listed in Tab. I, which are either rule-related or commonly used for learning-based algorithms, e.g., in [40], [41]. To avoid false negatives and false positives of the robustness prediction, i.e., to ensure

TABLE I: Feature variable definition. All values presented are in SI units and at time step k unless otherwise specified. To compute Δ_b or $\Delta_{\mathcal{L}^c}$, we use the signed distance from the vehicle center to its closest point at the road boundary b or the bounds of lane \mathcal{L}^c .

Feature Variable	Description
Rule-Related	
$c_p(\omega, k)$	characteristic function
Ego-Vehicle-Related	
$l_{\text{ego}}, w_{\text{ego}}$	vehicle length and width
$x_{\text{ego}}, u_{\text{ego}}$	state and input
$\Delta_{\mathcal{L}_1^c, \text{ego}}, \Delta_{\mathcal{L}_r^c, \text{ego}}$	left and right distance to the left and right boundary of the occupied lane
$\Delta_{b_l, \text{ego}}, \Delta_{b_r, \text{ego}}$	distance to the left and right road boundary
Other-Vehicle-Related	
l_b, w_b	vehicle length and width
x_b	state
$\Delta_{\mathcal{L}_1^c, b}, \Delta_{\mathcal{L}_r^c, b}$	left and right distance to the left and right boundary of the occupied lane
$\Delta_{b_l, b}, \Delta_{b_r, b}$	distance to the left and right road boundary
Ego-Other-Relative	
$\Delta s, \Delta d$	relative longitudinal and lateral distance
Δv	relative velocity

the soundness (cf. Prop. 1), we rectify the regression output using the characteristic function (cf. Def. 1) to obtain the estimated model predictive robustness $\tilde{\rho}_p^{\text{MP}}$ as:

$$\tilde{\rho}_p^{\text{MP}}(\omega, k) = \begin{cases} \widetilde{\max}(y^*, 0) & \text{if } c_p(\omega, k) = 1, \\ \widetilde{\min}(y^*, 0) & \text{if } c_p(\omega, k) = -1, \end{cases} \quad (7)$$

where the value of the predicted robustness with incorrect signs is set to 0 using the smooth minimum and maximum operators $\widetilde{\min}$ and $\widetilde{\max}$ defined in [16, (9) and (11)].

B. Evaluation on Properties

Tab. II summarizes the properties of the model-free and model predictive robustness. It shows that all desired properties listed in Sec. II-C are fulfilled by the model predictive robustness.

Theorem 1:

The model predictive robustness defined by (4) and combined with GP regression satisfies all properties 1-3.

Proof: The monotonicity and soundness of the model predictive robustness hold by definition. The smoothness of the robustness is fulfilled using the GP regression. A GP is fully specified by its mean and covariance (aka kernel) function. The mean is typically assumed to be zero in practice and we choose a squared-exponential kernel function, which is built on the assumption that feature variables close to each other (in terms of squared Euclidean distance) have similar robustnesses. The covariance between any two function values z_i and $z_{i'}$, $i, i' \in \{1, \dots, n_p\}$, is then given by [26, (6)]:

$$k(z_i, z_{i'}) = \sigma_\rho^2 \exp\left(\frac{1}{2}(z_i - z_{i'})^T L_\rho^{-1}(z_i - z_{i'})\right) + \delta(i, i')\sigma_\delta^2, \quad (8)$$

where L_ρ is the diagonal length-scale matrix with positive values, $\delta(\cdot)$ is the Kronecker delta function, and σ_ρ and σ_δ are the process deviation and discretization noise, respectively. The prediction of the regression model is a conditional probability distribution of y^* given \mathcal{D} , which remains a Gaussian distribution with $P(y^*|\mathcal{D}) = \mathcal{N}(\mu(z^*), \sigma^2(z^*))$ [24, Sec. 2.2] and

$$\begin{aligned} \mu(z^*) &= \mathbf{k}^T(z^*)\mathbf{K}^{-1}\mathbf{y}, \\ \sigma^2(z^*) &= \mathbf{k}(z^*, z^*) - \mathbf{k}^T(z^*)\mathbf{K}^{-1}\mathbf{k}(z^*). \end{aligned} \quad (9)$$

where $\mathbf{y} = [y_1, \dots, y_{n_p}]^T$ is the vector of observed outputs, $\mathbf{K} \in \mathbb{R}^{n_p \times n_p}$ is the covariance matrix with entries $K_{i,i'} = k(z_i, z_{i'})$, and $\mathbf{k}(z^*) = [k(z_1, z^*), \dots, k(z_{n_p}, z^*)]^T$ contains the covariances evaluated at all training data and observation

pairs. We take the mean $\mu(z^*)$ as the computed model predictive robustness, i.e., $y^* = \mu(z^*)$. Based on (8) and (9), y^* is a linear combination of the squared-exponential kernel functions contained in $\mathbf{k}(z^*)$, which are infinitely differentiable with respect to z^* [24, Sec. 4.2.1]. As a result, the model predictive robustness is smooth. Note that even if the rectification in (7) is used, the computed robustness is still sound and smooth (see [16, Thm. 1]). ■

With the deviation $\sigma(z^*)$ in (9), one can obtain the confidence intervals on the robustness computation. Since \mathbf{K} only needs to be inverted once for a given dataset, the complexities of evaluating the mean and variance in (9) are both $\mathcal{O}(n_p^2)$ [24, Alg. 2.1]. For applications with large amounts of data points, a sparse approximation of the GP regression [42] can be used to reduce the runtime complexity.

V. NUMERICAL EXPERIMENTS

We evaluate the applicability and efficacy of the model predictive robustness using the highD dataset [43] and German interstate traffic rules from [3], [8]. Our simulation is based on *CommonRoad* [44], and *GPyTorch* [45] is used to model and solve the GP regression. We use the vehicle model from [46, (8) and (13)], which separates the longitudinal and lateral motion of the vehicle in the curvilinear coordinate system (cf. Fig. 2). The trajectories for all rule-relevant vehicles described in Sec. III are determined with a time horizon of $h\Delta t = 1.5s$ with step size $\Delta t = 0.04s$. The number of the sampled trajectories for the ego vehicle is set to 1,000². The code used in this paper is published as open-source at <https://gitlab.lrz.de/tum-cps/mpr>. Our experiment videos can be accessed in the supplementary files of the paper.

A. GP Regression Model

Our robustness definition is validated by its usefulness against all predicates in the German interstate rules as referenced in [8]. We obtain 12,500 and 3,750 data points from the highD scenarios for predicates with $|\mathcal{B}| > 0$ and $|\mathcal{B}| = 0$, respectively. The data points are randomly divided into two sets, the training set and the test set, in a 4 : 1 ratio. All computations were executed using a single thread on a machine equipped with two AMD EPYC 7763 64-Core processors and 2TB RAM memory. The detailed evaluation results are summarized in Tab. III. The normalization values in (4) are obtained by evaluating the training set. The model predictive robustness of each predicate can be computed on average in less than 5ms. Moreover, we assess the performance of the GP regression model by examining its ability to correctly classify the satisfaction or violation of predicates on the test set. The precision, recall, and F1-score for the classification all have an average value of 0.9999. We can see that our proposed method maintains a high level of accuracy in robustness prediction, even without the rectification in (7).

²We independently sample the velocity, the lateral position, and the derivative of lateral position of the end states within the intervals $[v_k - 17.25, v_k + 17.25]$ in m/s, $[d_k - 5, d_k + 5]$ in m, and $[-3, 3]$ in m/s, respectively.

TABLE II: Comparison of fulfilled properties. Note that we examine the satisfaction of properties for all predicates.

Property	Model-free [8]	Model Predictive
Soundness	✓	✓
Smoothness	✗	✓
Monotonicity	✗	✓

TABLE III: Parameters and evaluation results for considered predicates. If there are no data points in the dataset that satisfy or violate the predicate, we set the normalization values $\bar{P}_{\pm, \min}$ and $\bar{P}_{\pm, \max}$ to 0 and 1, respectively.

Data	in_same_lane	single_lane	in_front_of
$\bar{P}_{+, \min}$	0.1935	0.2326	0.0526
$\bar{P}_{+, \max}$	0.9933	0.8076	1.0000
$\bar{P}_{-, \min}$	0.0000	0.0763	0.0000
$\bar{P}_{-, \max}$	0.9286	0.6072	0.9737
Comp. Time	4.07ms	3.99ms	4.12ms
Precision	0.9991	1.0000	1.0000
Recall	1.0000	1.0000	0.9992
F1-score	0.9995	1.0000	0.9996

Data	cut_in	keeps_safe_distance_prec	brakes_abruptly
$\bar{P}_{+, \min}$	0.0650	0.1959	0.3870
$\bar{P}_{+, \max}$	0.4575	1.0000	0.4154
$\bar{P}_{-, \min}$	0.0000	0.0000	0.2619
$\bar{P}_{-, \max}$	0.4347	0.7796	0.5794
Comp. Time	4.03ms	4.13ms	3.97ms
Precision	1.0000	1.0000	1.0000
Recall	1.0000	1.0000	1.0000
F1-score	1.0000	1.0000	1.0000

Data	brakes_abruptly_relative	keeps_lane_speed_limit	keeps_fov_speed_limit
$\bar{P}_{+, \min}$	0.3603	0.4942	0.0000
$\bar{P}_{+, \max}$	0.4862	1.0000	1.0000
$\bar{P}_{-, \min}$	0.1616	0.0646	0.0000
$\bar{P}_{-, \max}$	0.6862	0.5030	1.0000
Comp. Time	4.00ms	3.96ms	3.92ms
Precision	1.0000	1.0000	1.0000
Recall	1.0000	1.0000	1.0000
F1-score	1.0000	1.0000	1.0000

Data	keeps_type_speed_limit	keeps_brake_speed_limit
$\bar{P}_{+, \min}$	0.0000	0.6973
$\bar{P}_{+, \max}$	1.0000	1.0000
$\bar{P}_{-, \min}$	0.0000	0.1052
$\bar{P}_{-, \max}$	1.0000	0.4558
Comp. Time	3.94ms	3.96ms
Precision	1.0000	1.0000
Recall	1.0000	1.0000
F1-score	1.0000	1.0000

B. Comparison with Related Work

As discussed in Sec. IV-A, we consider comprehensive feature variables as inputs for the robustness prediction and can assess their predictive relevance utilizing the GP models. In contrast, the use of handcrafted functions to compute the robustness might lead to the lack of considered variables for complex predicates, which we demonstrate in the following example:

Example: Consider the predicate `in_same_lane` [3] which describes whether the ego vehicle shares a lane with the

vehicle $b \in \mathcal{B}$:

$$\text{in_same_lane} := |\mathcal{L}_{\text{ego}} \cap \mathcal{L}_b| > 0. \quad (10)$$

The calculation of its model-free robustness in [8, (1)] is sophisticated, but it only takes into account the positional attributes, represented as the signed distance to the lanes occupied by other vehicles. Domain-specific normalization constants are then used to confine the robustness within the interval $[-1, 1]$ [8, Tab. III]. However, as depicted in Fig. 4a, the model-free robustness remains close to zero after normalization. Instead, the model predictive robustness is easily normalized and spans the entire interval. Moreover, we use the variance of the GP posterior latent mean [47] to analyze the sensitivity of the feature variables. As shown in Fig. 4b, the distribution reveals that not only the relative distance to the lane bounds but also the relative velocity has a significant impact on the feature relevance. This is consistent with the human intuition of factors affecting the robustness of two vehicles maintaining the same lane, such as the variables used for calculating time-to-line-crossing [48, Tab. I].

C. Robustness-aware Trajectory Planning

Our robustness measure can be easily integrated into the prediction of traffic rule violations [8] and trajectory repairing [13]. In this section, we demonstrate that the model-predictive definition also facilitates the robustness aware-

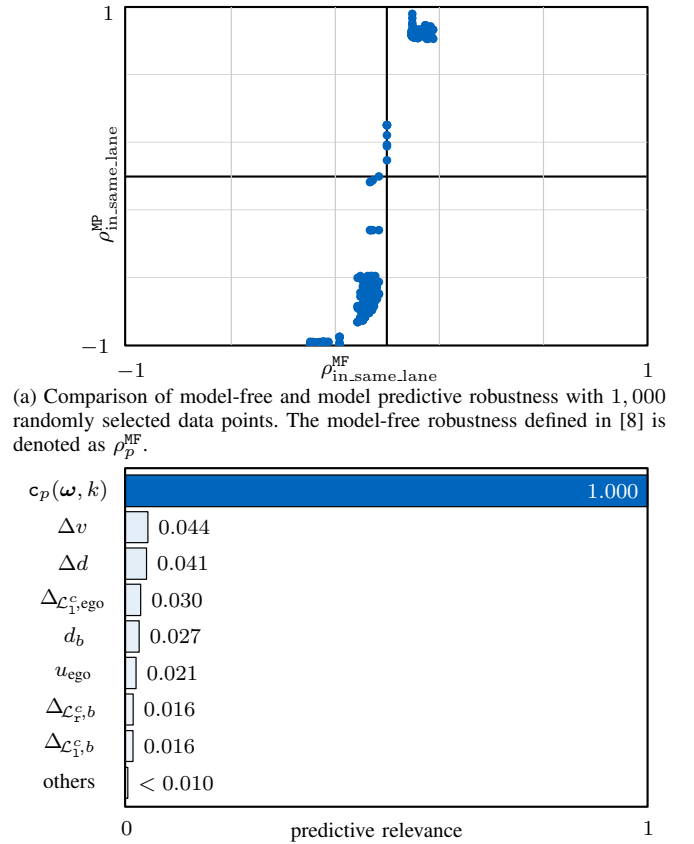


Fig. 4: Evaluation results of the predicate `in_same_lane`.

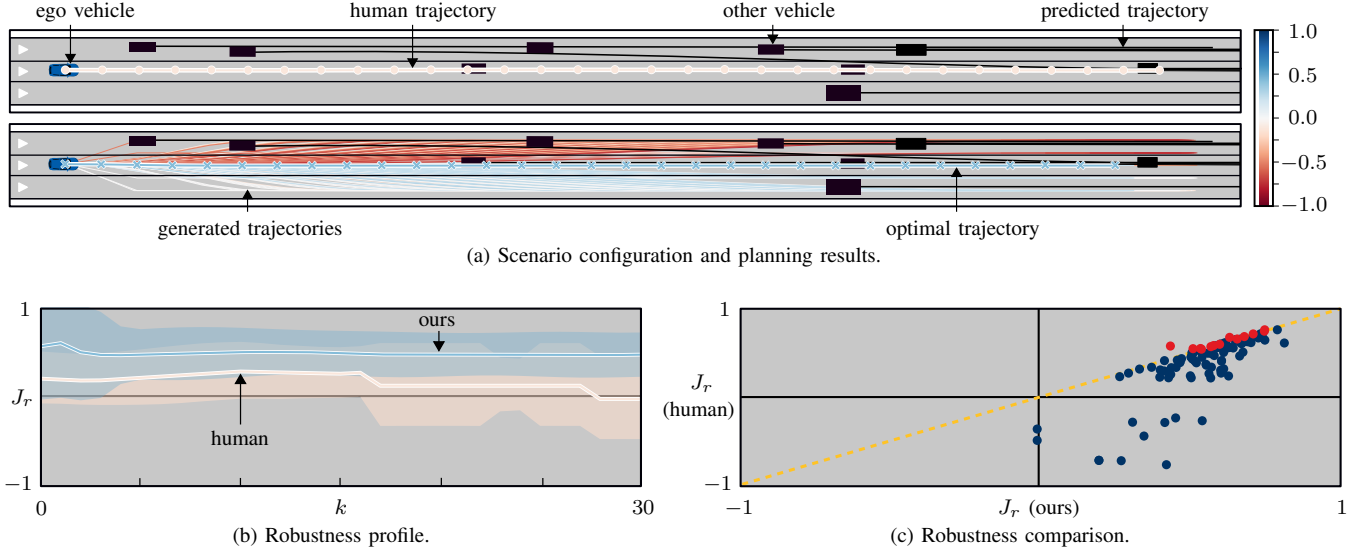


Fig. 5: Model-predictive-robustness-aware trajectory planning. The trajectories in (a) are color-coded according to the robustness, which increases from red with negative to blue with positive values. The shaded regions in (b) denote the $2\text{-}\sigma$ model uncertainty corresponding to a 95.4% confidence level. In (c), the blue dots to the right of the yellow dotted line indicate that the robustness of the optimal trajectory is higher than that of the human trajectory. The red dots to the left of the line indicate a lower robustness.

ness of trajectory planning using a sampling-based planner of [38]. The model predictive robustness of rules $\varphi_{R,G1}$ to $\varphi_{R,G3}$ ³ from [3] is integrated as an additional robustness term J_r with weight $\lambda_r \in \mathbb{R}_+$ in the cost function J to the planner:

$$J(x_{\text{ego},k}, u_{\text{ego},k}) = J_p(x_{\text{ego},k}, u_{\text{ego},k}) - \lambda_r J_r(x_{\text{ego},k}, u_{\text{ego},k}),$$

$$\text{s.t. } J_r(x_{\text{ego},k}, u_{\text{ego},k}) := \tilde{\rho}_{\varphi_{R,G1} \wedge \varphi_{R,G2} \wedge \varphi_{R,G3}}^{\text{MP}}(\omega, k),$$

where the performance term J_p is obtained from [38, (4)] and the robustness calculation of STL operators is based on [6, Def. 3]. During planning, the collision-free sample with the minimum cost is selected as the optimal trajectory.

We show an exemplary scenario in Fig. 5a, where 450 trajectories are generated with a time increment of $0.2s$ and a horizon of 30 time steps. The robustness distribution of the selected optimal trajectory is compared to the one of the recorded human trajectory in Fig. 5b. The human driver does not keep a safe distance to the preceding vehicle for $k \in [28, 30]$, i.e., the rule $\varphi_{R,G1}$ is violated. Including robustness as part of the cost function, the ego vehicle executes a braking maneuver to obey traffic rules as much as possible but with the least effort.

Furthermore, we evaluate the model-predictive-robustness-aware planning algorithm on 100 randomly selected highD scenarios. As shown in Fig. 5c, over 85% of the planned trajectories have greater robustness compared to the recorded ones, even when sampling only a finite subset of all possible trajectories. The results show that the model predictive robustness helps to enhance the degree of traffic rule compliance of autonomous vehicles, which significantly outperforms human drivers in the evaluated dataset. Due to the

systematic nature of our definition, incorporating additional rules with new predicates into the planner is straightforward.

VI. CONCLUSIONS

This paper examines how one can precisely and quickly quantify the level of satisfaction or violation of STL predicates considering the environment and dynamic models. Unlike existing model-free robustness definitions, our proposed model predictive robustness not only grows monotonically as the satisfaction probability increases but also is sound and smooth in the sense of Prop. 1-3. With this, our method can be useful in terms of rule-compliant planning and control for autonomous vehicles. Future work will focus on incorporating our definition into other STL variants and employing model predictive robustness in an optimization framework to synthesize controllers as well as repair rule-violating trajectories.

ACKNOWLEDGMENTS

The authors kindly thank Patrick Halder for his valuable suggestions on earlier drafts of this paper and Ethan Tatlow for the voice-over in the video attachment. The authors also gratefully acknowledge partial financial support by the German Federal Ministry for Digital and Transport (BMDV) within the project *Cooperative Autonomous Driving with Safety Guarantees* (KoSi).

REFERENCES

- [1] M. Luckcuck, M. Farrell, L. A. Dennis, C. Dixon, and M. Fisher, "Formal specification and verification of autonomous robotic systems: A survey," *ACM Computing Surveys*, vol. 52, no. 5, pp. 1–41, 2019.
- [2] K. Esterle, L. Gressenbuch, and A. Knoll, "Formalizing traffic rules for machine interpretability," in *Proc. of the IEEE Connected and Automated Veh. Symp.*, 2020, pp. 1–7.

³ $\varphi_{R,G1}$: Safe distance to preceding vehicle; $\varphi_{R,G2}$: Unnecessary braking; $\varphi_{R,G3}$: Maximum speed limit.

- [3] S. Maierhofer, A.-K. Rettinger, E. C. Mayer, and M. Althoff, "Formalization of interstate traffic rules in temporal logic," in *Proc. of the IEEE Intell. Veh. Symp.*, 2020, pp. 752–759.
- [4] N. Aréchiga, "Specifying safety of autonomous vehicles in signal temporal logic," in *Proc. of the IEEE Intell. Veh. Symp.*, 2019, pp. 58–63.
- [5] G. E. Fainekos and G. J. Pappas, "Robustness of temporal logic specifications for continuous-time signals," *Theoretical Computer Science*, vol. 410, no. 42, pp. 4262–4291, 2009.
- [6] A. Donzé and O. Maler, "Robust satisfaction of temporal logic over real-valued signals," in *Proc. of the Int. Conf. on Formal Modeling and Analysis of Timed Syst.*, 2010, pp. 92–106.
- [7] E. Bartocci, J. Deshmukh, A. Donzé, G. Fainekos, O. Maler, D. Ničković, and S. Sankaranarayanan, "Specification-based monitoring of cyber-physical systems: A survey on theory, tools and applications," in *Lectures on Runtime Verification*. Cham: Springer, 2018, pp. 135–175.
- [8] L. Gressenbuch and M. Althoff, "Predictive monitoring of traffic rules," in *Proc. of the IEEE Int. Conf. on Intell. Transp. Syst.*, 2021, pp. 915–922.
- [9] S. Maierhofer, P. Moosbrugger, and M. Althoff, "Formalization of intersection traffic rules in temporal logic," in *Proc. of the IEEE Intell. Veh. Symp.*, 2022, pp. 1135–1144.
- [10] H. Krasowski and M. Althoff, "Temporal logic formalization of marine traffic rules," in *Proc. of the IEEE Intell. Veh. Symp.*, 2021, pp. 186–192.
- [11] M. Hekmatnejad, S. Yaghoubi, A. Dokhanchi, H. B. Amor, A. Shrivastava, L. Karam, and G. Fainekos, "Encoding and monitoring responsibility sensitive safety rules for automated vehicles in signal temporal logic," in *Proc. of the ACM/IEEE Int. Conf. on Formal Methods and Models for Syst. Design*, 2019, pp. 1–11.
- [12] W. Xiao, N. Mehdipour, A. Collin, A. Y. Bin-Nun, E. Frazzoli, R. D. Tebbens, and C. Belta, "Rule-based optimal control for autonomous driving," in *Proc. of the ACM/IEEE Int. Conf. on Cyber-Physical Syst.*, 2021, pp. 143–154.
- [13] Y. Lin and M. Althoff, "Rule-compliant trajectory repairing using satisfiability modulo theories," in *Proc. of the IEEE Intell. Veh. Symp.*, 2022, pp. 449–456.
- [14] Y. V. Pant, H. Abbas, and R. Mangharam, "Smooth operator: Control using the smooth robustness of temporal logic," in *Proc. of the IEEE Conf. on Control Technology and Applications*, 2017, pp. 1235–1240.
- [15] N. Mehdipour, C.-I. Vasile, and C. Belta, "Arithmetic-geometric mean robustness for control from signal temporal logic specifications," in *Proc. of the IEEE American Control Conf.*, 2019, pp. 1690–1695.
- [16] Y. Gilpin, V. Kurtz, and H. Lin, "A smooth robustness measure of signal temporal logic for symbolic control," *IEEE Control Syst. Letters*, vol. 5, no. 1, pp. 241–246, 2020.
- [17] P. Varnai and D. V. Dimarogonas, "On robustness metrics for learning STL tasks," in *Proc. of the IEEE American Control Conf.*, 2020, pp. 5394–5399.
- [18] V. Kurtz and H. Lin, "Mixed-integer programming for signal temporal logic with fewer binary variables," *IEEE Control Syst. Letters*, vol. 6, pp. 2635–2640, 2022.
- [19] C. Yoo and C. Belta, "Control with probabilistic signal temporal logic," *arXiv preprint arXiv:1510.08474*, 2015.
- [20] D. Sadigh and A. Kapoor, "Safe control under uncertainty with probabilistic signal temporal logic," in *Proc. of Robotics: Science and Syst. XII*, 2016.
- [21] M. Tiger and F. Heintz, "Incremental reasoning in probabilistic signal temporal logic," *Int. J. of Approximate Reasoning*, vol. 119, pp. 325–352, 2020.
- [22] K. M. B. Lee, C. Yoo, and R. Fitch, "Signal temporal logic synthesis as probabilistic inference," in *Proc. of the IEEE Int. Conf. on Robotics and Automation*, 2021, pp. 5483–5489.
- [23] T. Nyberg, C. Pek, L. Dal Col, C. Norén, and J. Tumova, "Risk-aware motion planning for autonomous vehicles with safety specifications," in *Proc. of the IEEE Intell. Veh. Symp.*, 2021, pp. 1016–1023.
- [24] C. E. Rasmussen and C. K. Williams, *Gaussian processes for machine learning*. Cambridge: MIT press, 2006.
- [25] J. Kocijan, R. Murray-Smith, C. E. Rasmussen, and A. Girard, "Gaussian process model based predictive control," in *Proc. of the IEEE American Control Conf.*, 2004, pp. 2214–2219.
- [26] F. Berkenkamp and A. P. Schoellig, "Safe and robust learning control with Gaussian processes," in *Proc. of the IEEE European Control Conf.*, 2015, pp. 2496–2501.
- [27] L. Hewing, J. Kabzan, and M. N. Zeilinger, "Cautious model predictive control using Gaussian process regression," *IEEE Trans. on Control Syst. Technology*, vol. 28, no. 6, pp. 2736–2743, 2019.
- [28] T. R. Torben, J. A. Glomsrud, T. A. Pedersen, I. B. Utne, and A. J. Sørensen, "Automatic simulation-based testing of autonomous ships using Gaussian processes and temporal logic," *Proc. of the Institution of Mechanical Engineers, Part O: J. of Risk and Reliability*, 2022.
- [29] E. Héry, S. Masi, P. Xu, and P. Bonnifait, "Map-based curvilinear coordinates for autonomous vehicles," in *Proc. of the IEEE Int. Conf. on Intell. Transp. Syst.*, 2017, pp. 1–7.
- [30] E. F. Camacho and C. B. Alba, *Model predictive control*. Springer science & business media, 2013.
- [31] P. Schneider, M. Butz, C. Heinzemann, J. Oehlerking, and M. Woehrle, "Towards threat metric evaluation in complex urban scenarios," in *Proc. of the IEEE Intell. Transp. Syst. Conf.*, 2021, pp. 1192–1198.
- [32] D. Koller and N. Friedman, *Probabilistic graphical models: principles and techniques*. MIT press, 2009.
- [33] K. P. Murphy, *Dynamic Bayesian networks: Representation, inference and learning*. University of California, Berkeley, 2002.
- [34] M. Althoff, O. Stursberg, and M. Buss, "Model-based probabilistic collision detection in autonomous driving," *IEEE Trans. on Intell. Transp. Syst.*, vol. 10, no. 2, pp. 299–310, 2009.
- [35] A. Spanos, *Probability theory and statistical inference: Empirical modeling with observational data*. Cambridge University Press, 2019.
- [36] A. Broadhurst, S. Baker, and T. Kanade, "Monte Carlo road safety reasoning," in *Proc. of the IEEE Intell. Veh. Symp.*, 2005, pp. 319–324.
- [37] T. M. Howard, C. J. Green, A. Kelly, and D. Ferguson, "State space sampling of feasible motions for high-performance mobile robot navigation in complex environments," *J. of Field Robotics*, vol. 25, no. 6-7, pp. 325–345, 2008.
- [38] M. Werling, S. Kammel, J. Ziegler, and L. Gröll, "Optimal trajectories for time-critical street scenarios using discretized terminal manifolds," *The Int. J. of Robotics Research*, vol. 31, no. 3, pp. 346–359, 2012.
- [39] C. Pek, V. Rusinov, S. Manzingier, M. C. Üste, and M. Althoff, "CommonRoad Drivability Checker: Simplifying the development and validation of motion planning algorithms," in *Proc. of the IEEE Intell. Veh. Symp.*, 2020, pp. 1013–1020.
- [40] X. Wang, H. Krasowski, and M. Althoff, "Commonroad-RL: A configurable reinforcement learning environment for motion planning of autonomous vehicles," in *Proc. of the IEEE Int. Conf. on Intell. Transp. Syst.*, 2021, pp. 466–472.
- [41] T. Gindele, S. Brechtel, and R. Dillmann, "A probabilistic model for estimating driver behaviors and vehicle trajectories in traffic environments," in *Proc. of the IEEE Int. Conf. on Intell. Transp. Syst.*, 2010, pp. 1625–1631.
- [42] J. Quinero-Candela and C. E. Rasmussen, "A unifying view of sparse approximate Gaussian process regression," *The J. of Machine Learning Research*, vol. 6, pp. 1939–1959, 2005.
- [43] R. Krajewski, J. Bock, L. Kloecker, and L. Eckstein, "The highD dataset: A drone dataset of naturalistic vehicle trajectories on German highways for validation of highly automated driving systems," in *Proc. of the IEEE Int. Conf. on Intell. Transp. Syst.*, 2018, pp. 2118–2125.
- [44] M. Althoff, M. Koschi, and S. Manzingier, "CommonRoad: Composable benchmarks for motion planning on roads," in *Proc. of the IEEE Intell. Veh. Symp.*, 2017, pp. 719–726.
- [45] J. Gardner, G. Pleiss, K. Q. Weinberger, D. Bindel, and A. G. Wilson, "GPpyTorch: Blackbox matrix-matrix Gaussian process inference with GPU acceleration," in *Proc. of the Conf. on Neural Information Processing Syst.*, 2018, pp. 7576–7586.
- [46] C. Pek and M. Althoff, "Fail-safe motion planning for online verification of autonomous vehicles using convex optimization," *IEEE Trans. on Robotics*, vol. 37, no. 3, pp. 798–814, 2021.
- [47] T. Paaananen, J. Piironen, M. R. Andersen, and A. Vehtari, "Variable selection for Gaussian processes via sensitivity analysis of the posterior predictive distribution," in *Proc. of the Int. Conf. on Artificial Intell. and Statistics*, 2019, pp. 1743–1752.
- [48] S. Mammars, S. Glaser, and M. Netto, "Time to line crossing for lane departure avoidance: A theoretical study and an experimental setting," *IEEE Trans. on Intell. Transp. Syst.*, vol. 7, no. 2, pp. 226–241, 2006.